Triboelectric generation by friction of heavily doped diamond probes on a *p*-Si surface

© P.A. Alekseev, D.D. Sakhno, M.S. Dunaevskiy

Ioffe Institute,
194021 St. Petersburg, Russia
E-mail: npoxep@gmail.com

Received October 27, 2023
Revised November 20, 2023
Accepted November 22, 2023

The generation of triboelectric current during friction of diamond probes on the surface of *p*-Si substrates with a native oxide layer was studied. The choice of probes with different doping, as well as substrates with different surface orientations, made it possible to establish the determining influence of the probe-surface work functions difference on the direction and value of the triboelectric current. The generation of triboelectric current occurs due to the tunneling of non-equilibrium charge carriers resulting from the chemical bonds breaking during friction. Under illumination conditions, an increase in the triboelectric current was observed, as well as the photocurrent appearance due to the charge carriers separation in the space charge region.

Keywords: triboelectricity, triboelectric generation, silicon, doped diamond, tunneling, photocurrent.

DOI: 10.61011/SC.2023.09.57432.5701

1. Introduction

The creation of miniature devices for converting the mechanical energy of the environment into electricity is a relevant task. One approach is to use the triboelectric effect, which consists in charge transfer during frictional contact of different materials. An active study of triboelectric generation in case of friction of dielectric materials made it possible to increase the power density of such generators to 500 W/m^2 and achieve a mechanical energy conversion efficiency of 50% [1]. The friction of dielectric materials generates displacement currents in the circuit and such generators produce high voltages and relatively low alternating currents $\sim 0.1\,A/m^2$ [2]. The approach of using semiconductor materials in triboelectric generators has recently been developed to increase the output current [3]. Current densities $10^5\,A/m^2$ [4] are achieved in case of friction of conductive electrode against the surface of high doped Si. At the same time, these generators produce a current with a constant direction. The mechanism of triboelectric current generation in case of friction against a semiconductor is debatable [3]. For the current generation an electric field should be present in the area of the frictional contact. Such a field can be attributable to the difference of work function, the flexoelectric effect of [5], the appearance and destruction of electric dipoles [6] in the boundary region. The friction of materials is a non-adiabatic process and in the contact area, electron-hole pairs are generated due to the rupture of chemical bonds [7]. It is important to note that the polarity of the triboelectric current during friction of the same pairs of materials in different works may be different. The current can be either positive [8] or negative in case of friction of an Au electrode against *p*-Si [9]. The exact reasons for this difference have not been determined and additional studies are required.

Scanning probe microscopy (SPM) is one of the main tools for the study of triboelectric generation in semiconductors [3]. Indeed, the SPM allows controlling the amount of pressure on the surface, the contact area and the speed of movement of the probe during friction. The use of probes with different conductive coatings allows changing the difference of work functions. In addition, using SPM it is possible to study the topographic and electrical properties of the surface before and after friction. On the other hand, there are a number of disadvantages of SPM for studying triboelectric generation. Most modern atomic force microscopes use an optical system to detect the position of the probe, which leads to the illumination of the surface with laser radiation [10]. Such illumination, with the quantum of energy of optical radiation greater than the band gap of the semiconductor ($h\omega > E_g$), will result in additional effects — photopotential and photoconductivity. Unfortunately, the impact of these effects is ignored in some studies [11].

Another challenge is the selection of a probe with a conductive coating. The following commercially available conductive probes are known: (i) with a conductive coating (Au, PtIr, Al, W_2C, TiN), (ii) all-metal (Pt) and (iii) wear-resistant with a solid diamond needle or polycrystalline diamond coating. The conductive coatings wear out during friction, and the all-metal Pt needle deforms under strong pressure, changing the contact area. Therefore, the use of high doped diamond is the best option. It is important to note that there are commercially available probes with a solid diamond needle doped with boron (*p*-type, DEP30, NT-MDT probes), as well as with a polycrystalline coating doped with nitrogen (*n*-type, DCP11, NT-MDT probes). Despite the fact that diamond is a wide-band semiconductor with a band gap of 5.5 eV, a high level of doping creates

Triboelectric current and surface potential values for various pairs of semiconductor materials

	KDB001 (100) WF = 4.85 ± 0.1 eV *I*, pA		KDB005 (111) WF = 4.65 ± 0.1 eV *I*, pA		KDB12 (100) WF = 4.65 ± 0.1 eV *I*, pA		KDB001 (100) SP, mV	KDB005 (111) SP, mV
	dark	light	dark	light	dark	light	dark	dark
DCP11, *n*-type, WF = 4.68 ± 0.1 eV	12 ± 6	−200 ± 100	−20 ± 30	1000 ± 700	0 ± 3	−1000 ± 500	50 ± 100	300 ± 100
DEP30, *p*-type, WF = 4.78 ± 0.1 eV	4000 ± 3000	7000 ± 4000	0 ± 10	0 ± 100	0 ± 3	−50 ± 30	−50 ± 100	200 ± 100

an impurity conductive band and when such probes come into contact with a metal surface, the I-V curves have a linear shape [12,13]. However, the difference of the work function (WF) of these probes is ∼ 100 meV [14]. Thus, the use of these probes makes it possible to study the impact of the difference of work function on the value and polarity of the triboelectric current. In addition, it is known that the substrates *p*-Si also have different work function values depending on the orientation of the surface ((100) or (111)) [15] and generate current pulses of opposite polarity when in contact with the conductive probe [16].

Aims of this work are: (i) to study the value and polarity of the triboelectric current depending on the difference of work function in case of friction of probes with a highly doped diamond coating on a substrate *p*-Si with different surface orientation, (ii) to determine the mechanism of triboelectric current generation and identify the impact of optical excitation on the generated current.

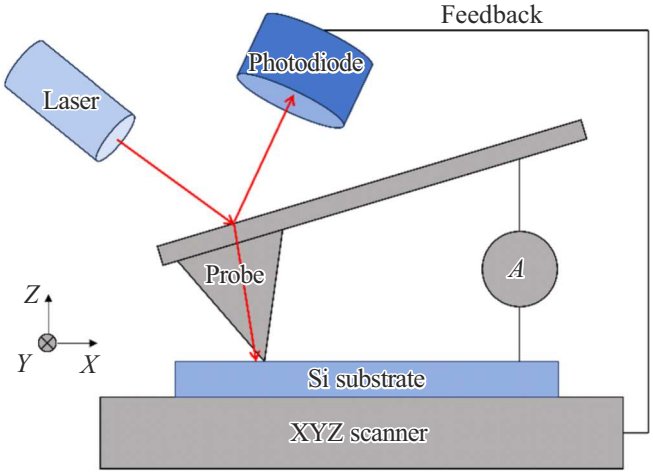

Figure 1. Experimental scheme for measuring triboelectric current.

2. Samples and methods

Silicon substrates KDB001 with a surface of (100), KDB005 with a surface of (111) and silicon substrates KDB12 with a surface of (100) were studied in this paper. The substrates were doped with boron and the doping levels were respectively $1 \cdot 10^{20}$, $5 \cdot 10^{19}$, $1 \cdot 10^{16}$ cm^{-3} (see table). The substrates had a layer of native oxide with a thickness of ∼ 1 nm with a surface roughness RMS (root mean square) 0.2 nm.

Triboelectric generation studies were performed using conductive atomic force microscopy with NTEGRA AURA SPM (NT-MDT, Russia). DEP30 (NT-MDT, Russia), doped with boron, and DCP11 (NT-MDT, Russia), doped with nitrogen were used as probes. The stiffness of the DEP30 cantilevers was 20 N/m, and the stiffness of the DCP11 cantilevers was — 10 N/m. Triboelectric current was recorded by an integrated ammeter with a sensitivity of 3 pA. It is important to note that, as a rule, scanning in contact mode is conducted in constant force mode. The feedback sends control signals to the Z-scanner (moving up and down) at each point of the surface to maintain the constant bending of the beam (cantilever), and therefore to maintain at a constant level the pressure force (Figure 1). The degree of bending of the beam is controlled using a laser-photodiode optical system. This configuration results in a partial illumination of the sample surface by a laser with a wavelength of 650 nm. The SPM used in the work allows switching off the laser and feedback and creating contact between the probe and the surface by changing the position of the Z-scanner. Since the surface plane of the sample may not be parallel to the scanning plane *XY*, the pressure force on the surface will vary according to the angle of inclination of the surface. This angle ($< 2^\circ$) in the study was minimized by changing the inclination of the sample. In addition, triboelectric currents occurred only in case of strong pressure of the probe on the surface ($\Delta z > 500$ nm relative to the initial touch of the surface point), therefore, the impact of the inclination of the sample plane can be ignored. Triboelectric current was recorded by scanning the area $1 \times 1\,\mu m^2$ at a speed of 1 line per second with a resolution of 128 × 128 points.

The magnitude of the electric field in the probe-substrate contact area depends on the difference between the work function of the probe and the substrate (surface potential). The measurement of the surface potential (SP) was performed using the Kelvin probe microscopy method with an 1300 nm IR laser. It is important to note that in case of friction, the surface work function may differ from the work

function measured by Kelvin-probe microscopy due to the presence of a film of aqueous adsorbate on the surface, the flexoelectric effect, as well as fluctuations in the local work function. The study of the effect of illumination on the triboelectric current was performed by switching on or off the built-in laser (Figure 1).

3. Results and discussion

Figure 2, *a* shows the topography of the surface of the KDB001 sample obtained in semi-contact mode using the DEP30 probe. The direction of the slow scan corresponds to the horizontal axis on the scan. A triboelectric current map was measured after obtaining an image of the surface topography, (Figure 2, *b*). Scanning of the initial area with a length of 200 nm (dark vertical stripe) was performed without creating a mechanical contact. Then the probe was brought into contact with the surface with a pressure force of 10 μN, and triboelectric current was generated in the circuit. The characteristic profile of the triboelectric current obtained along the dotted line in Figure 2, *b* is shown in Figure 2, *c*. The current value for this probe-substrate pair in dark conditions is 4 ± 3 nA. A positive current value corresponds to the movement of electrons from the probe into the substrate. Current was generated only during the friction of the probe against the surface. There was no current when the probe was stopped (in dark conditions). It is important to note that the triboelectric current occurred only with strong pressure on the surface (with force $F > 1\,\mu$N), and a depression was observed in the scanning area after obtaining the triboelectric current map. Apparently, chemical bonds on the surface did not break with weaker forces and no energy was release sufficient to produce charge carriers carrying current. The triboelectric current disappeared if the depth of the depression exceeded the thickness of the surface native oxide.

Thus, triboelectric generation occurred only in case of partial destruction of the surface oxide. A detailed study of the mechanical degradation of the surface in case of triboelectric generation is beyond the scope of this work and the pressure force on the surface was maintained at the level of 10 μN for the convenience of comparing the values of triboelectric current.

The table below shows the values of the triboelectric current for the probes and substrates under study in conditions of darkness and laser illumination.

It follows from the table that the value of the triboelectric current, depending on the probe and the substrate, can vary by several orders of magnitude. Moreover, the polarity of the current may change when the laser illumination is switched on. It is interesting to note that the current polarity can be variable in the same conditions for a number of probe-substrate pairs (KDB005). In dark conditions, no triboelectric current was recorded for the low doped KDB12 substrate. Taking into account the sensitivity of the ammeter used, the obtained values are consistent with the data presented in the works for silicon with the same level and type of doping [11].

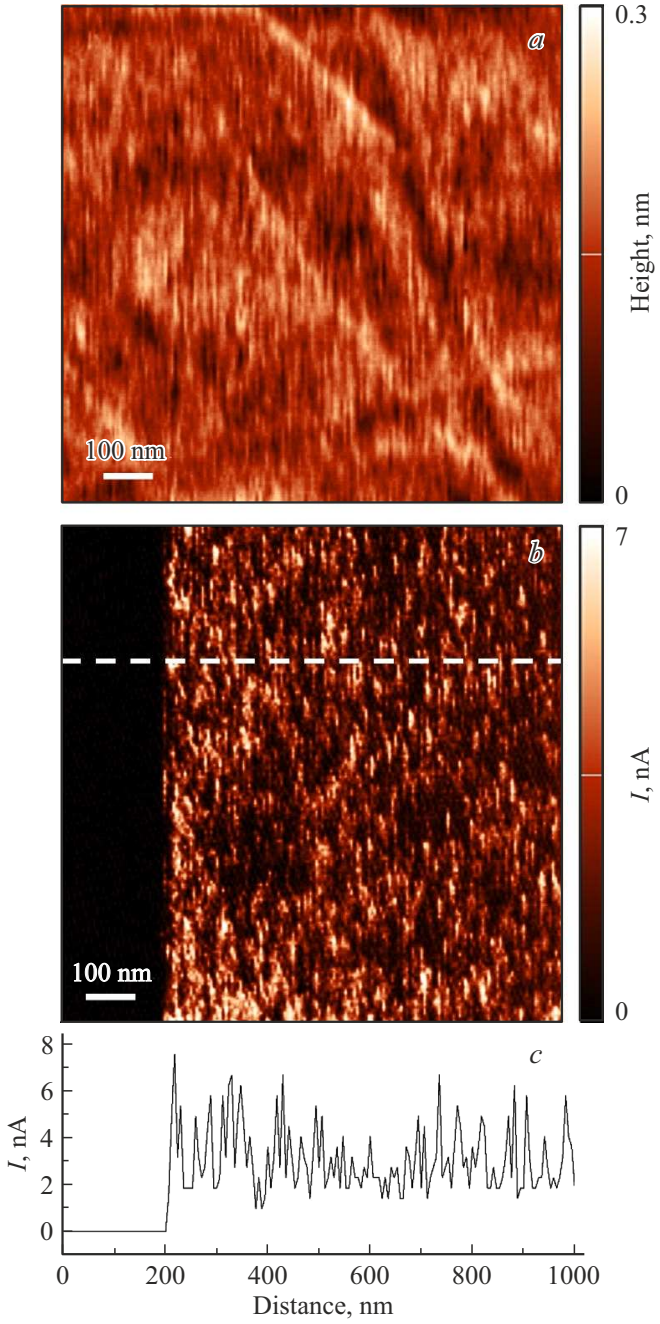

Figure 2. Study of the KDB001 substrate with the DEP30 probe (*p*-type): *a* — surface topography; *b* — triboelectric current map. The contact between the probe and the surface was created when the horizontal coordinate 200 nm was reached; *c* — the triboelectric current profile along the dotted line in Figure *b*. (The colored version of the figure is available on-line).

We consider the energy diagrams of the probes and the semiconductors under study to explain the experimental data obtained. As already mentioned above, the triboelectric current may be attributable to the difference between the

work function of the probe and the substrate surface. The values of the work functions of the probes DCP11 and DEP30 are presented in the article [14], in which the work function of the probes was determined by comparing it with the work function of highly oriented pyrolytic graphite (HOPG). However, an incorrect value was used for the operation of the work function of HOPG 4.6 ± 0.1 eV. The correct value is 4.48 eV [17]. Thus, the work function of the probe DEP30 should be 4.78 ± 0.1 eV, and the work function probe DCP11 should be 4.68 ± 0.1 eV. The difference of 0.1 eV is consistent with the surface potential data presented in the table. The work function is 4.85 ± 0.1 eV for p-Si (100) and 4.6 ± 0.1 eV for p-Si (111) [15]. This difference is also consistent with the surface potential measurements presented in the table. It is important to note that the electron affinity of silicon is 4.05 eV, which leads to a near-surface band bending, since the position of the Fermi level in the bulk does not coincide with the Fermi level on the surface (work function) pinned on the surface states. In addition, a high level of doping in the bulk Si leads to a shift in the Fermi level by 60 meV below the bottom of the conduction band in KDB001 and 40 meV in KDB005. Taking into account the doping level and the position of the Fermi level on the surface, the width of the near-surface depletion region for KDB005 is 4 nm, and 1.5 nm for KDB 001.

The band diagrams in the surface oxide region for KDB001 and KDB005, respectively, are shown on Figure 3, *a* and *b*. The positions of the Fermi levels and charge carriers are shown in black in case of dark conditions and in case of red laser illumination. The figure also shows the work function of the DEP30 and DCP11 probes. The figure is provided for the case when there was no electrical contact between the probe and the surface and the Fermi levels were not aligned. It is important to note that boron and nitrogen in diamond are sufficiently deep impurities 0.3 and 1.7 eV [18], respectively, and therefore the position of the valence band and the conduction band of diamond at room temperature can be ignored. However, it is important to take into account that high doping creates an impurity band of finite width in the band gap.

Let's consider the case of friction of the DCP11 probe against the KDB001 substrate (Figure 3, *a*). Energy which can lead to the formation of electron-hole pairs is released in case of friction in the contact area due to the rupture of chemical bonds or heating of the crystal lattice. In addition, the doped probe also has a high concentration of charge carriers. The relative position of the Fermi levels of the probe and the substrate makes it possible to directly tunnel electrons from the probe only to the surface states at the silicon/surface oxide interface. The exchange of charges of these states with the volume of silicon is complicated since direct tunneling into the band gap is not possible. However, if we consider the case for the DEP30 probe, in which the Fermi level is lower by ~ 100 meV, then tunneling into the valence band becomes possible, and therefore the value of the triboelectric current increases by 3 orders of magnitude

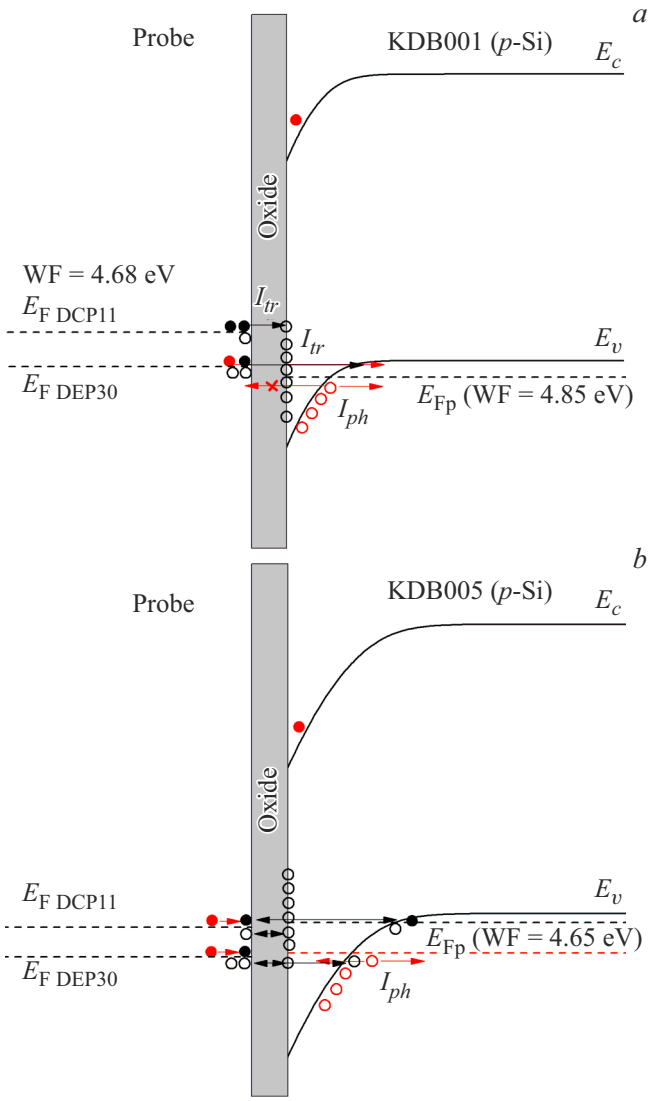

Figure 3. Energy band diagrams in the surface oxide region for KDB001 (*a*) and KDB005 (*b*). Black circles — distribution of carriers in the dark conditions, red circles — distribution of carriers with illumination. Filled circles — electrons, unfilled circles — holes. (The colored version of the figure is available on-line).

(see table). The polarity of the recorded current also corresponds to the tunneling of electrons from the probe into silicon.

The concentration of nonequilibrium charge carriers increases in illumination conditions, a near-surface depletion region narrows and Fermi quasi-level shifts downwards for holes. However, it should be borne in mind that the contribution of laser illumination will be less the higher the silicon doping level, since the intensity of laser radiation reaching the substrate is low and corresponds to $\sim 10^4$ W/m^2 [19]. Thus, a photocurrent (I_{ph}) will occur in KDB001/DCP11 pair, in case of illumination, in addition to preservation of the tunneling of electrons from the probe to surface states (I_{tr}) during the separation of electron-hole

pairs in the near-surface depletion region. In this case, the holes will move into the semiconductor, which corresponds to a negative current. It is important to note that direct tunneling of holes into the probe is also impossible, due to the narrowness of the impurity band in the diamond. The prevalence of the photocurrent over the triboelectric current results in the negative direction of the total current. In the case of KDB001/DEP30, the possibility of direct tunneling of both electrons from the probe into the valence band and holes into the probe leads to an additional increase of the recorded current compared to dark conditions.

A different pattern is observed in the KDB005 substrate due to the proximity of the Fermi levels of the probes and the substrate. In addition, the wider depletion region significantly reduces tunnel currents. Under dark conditions, the recorded current has relatively low values in case of both probes and has an alternative direction at different points of the scan, which is explained by local fluctuations of the relative positions of the Fermi levels. The current is lower in case of the DEP30 probe, since the difference with the Fermi level in the substrate is more significant 130 ± 200 meV, compared with 30 ± 200 meV in case of the DCP11 probe. The Fermi quasi-level for holes shifts downwards in illumination conditions, which increases the probability of electron tunneling from the DCP11 probe into the substrate. This configuration is similar to the configuration for the KDB001/DEP30 pair (Figure 3, *a*), so the current has a positive direction. The Fermi levels almost coincide in illumination conditions in the KDB005/DEP30 pair, which leads to the generation of a current with alternating polarity, but an increased amplitude compared to dark conditions due to nonequilibrium charge carriers and narrowing of the depletion region. The behavior of nonequilibrium electrons in the conduction band of silicon was not discussed in the cases considered above. The near-surface band bending and the larger distance from the Fermi level, compared with holes, lead to low electron currents in the Si conduction band, which can be neglected.

In case of the KDB12 substrate, the bulk Fermi level is in the band gap and low doping leads to a significant broadening of the depletion region, and decrease of tunneling current and leads to the absence of triboelectric generation. The probe–substrate contact works as a solar cell in illumination conditions and the photocurrent has a negative direction.

The analysis of the experimental results allows formulating several rules affecting the value of the triboelectric current at the frictional contact of two high doped semiconductors.

The polarity of the triboelectric current in dark conditions is determined by the difference of work function (the position of Fermi level pinning on the surface). The polarity is not determined by the p–n-electric field of the junction, as was postulated in the tribovoltaic effect model [11].

Triboelectric generation occurs in high doped semiconductors with a layer of native oxide, which confirms the mechanism of triboelectric tunneling [8]. The surface states at the oxide/semiconductor interface are necessary as intermediate states through which triboelectric current flows.

Triboelectric generation was observed only in the case of topographic changes on the surface. Thus, energy is released due to the destruction and formation of chemical bonds on the surface of the oxide [4].

Both an increase of triboelectric current takes place in illumination conditions due to increased tunneling, and the photocurrent is produced due to the separation of nonequilibrium carriers in the near-surface depletion region. The triboelectric current and the photocurrent can have opposite polarities and the total current is determined by the balance of these currents.

4. Conclusion

The current generation in case of friction of high doped diamond probes of *p*- and *n*-type of doping on the surface of *p*-Si with different doping levels and surface orientation was studied in this paper. The work function of the probe of *n*-type was 100 meV less than the work function of the probe of *p*-type of doping. The work function of *p*-Si (100) was 250 meV greater than work function of *p*-Si (111). These differences of the work function of the probes and Si substrates allowed studying the effect of the difference of work functions on the direction and magnitude of the triboelectric current.

The generation of triboelectric current was observed in dark condition in case of friction of the probe against the surface of high-doped *p*-Si. The direction of the current was determined by the difference between the work function of the probe and the surface, and the current flowed to the material with a lower work function. Triboelectric generation was attributable to the release of energy when the probe destroyed chemical bonds on the surface. The release of energy leads to the generation of nonequilibrium charge carriers that tunnel through the surface oxide and near-surface depletion region in silicon. The magnitude of the triboelectric current is determined by the width of the near-surface depletion region and the possibility of direct tunneling of charge carriers into the valence band. So, for example, for a pair of diamond probe of *n*-type–substrate KDB001 (100) the Fermi level of the probe falls into the band gap in Si and the triboelectric current is 12 ± 6 pA, while for of the probe of *p*-type, the Fermi level falls into the valence band and the current increases by 3 orders — to 4 ± 3 nA.

The triboelectric current increases in illumination conditions, due to nonequilibrium charge carriers and a decrease of the width of the near-surface depletion region. However, an additional photocurrent is generated due to the field of the near-surface depletion region and the direction of this current may not coincide with the direction of the triboelectric current. The total friction current in lighting conditions is determined by the balance of triboelectric and

photocurrents. The results of the work will increase the efficiency of triboelectric generators based on semiconductor materials, as well as hybrid devices triboelectric generator-solar cell.

Funding

The study was supported by a grant from the Russian Science Foundation no. 22-22-20084 (https://rscf.ru/project/22-22-20084/) and a grant from the St. Petersburg Science Foundation in accordance with the agreement dated April 14, 2022, no. 24/202,2.

Conflict of interest

The authors declare that they have no conflict of interest.

References

[1] G. Zhu, Y.S. Zhou, P. Bai, X.S. Meng, Q. Jing, J. Chen, Z.L. Wang. Advanced Mater., **26** (23), 3788 (2014).
[2] Z.L. Wang. Materials Today, **20** (2), 74 (2017).
[3] R. Yang, R. Xu, W. Dou, M. Benner, Q. Zhang, J. Liu. Nano Energy, **83**, 105849 (2021).
[4] S. Lin, R. Shen, T. Yao, Y. Lu, S. Feng, Z. Hao, H. Zheng, Y. Yan, E. Li. Advanced Sci., **6** (24), 1901925 (2019).
[5] P. Yudin, A. Tagantsev. Nanotechnology, **24** (43), 432001 (2013).
[6] K.M. Abdelaziz, J. Chen, T.J. Hieber, Z.C. Leseman. J. Electrostatics, **96**, 10 (2018).
[7] J.Y. Park, M. Salmeron. Chem. Rev., **114** (1), 677 (2014).
[8] J. Liu, M. Miao, K. Jiang, F. Khan, A. Goswami, R. McGee, Z. Li, L. Nguyen, Z. Hu, J. Lee, K. Cadien, T. Thundat. Nano Energy, **48**, 320 (2018).
[9] S. Lin, Y. Lu, S. Feng, Z. Hao, Y. Yan. Advanced Mater., **31** (7), 1804398 (2019).
[10] V.A. Sharov, P.A. Alekseev, B.R. Borodin, M.S. Dunaevskiy, R.R. Reznik, G.E. Cirlin. ACS Appl. Energy Mater., **2** (6), 4395 (2019).
[11] M. Zheng, S. Lin, L. Xu, L. Zhu, Z.L. Wang. Advanced Mater., **32** (21), 2000928 (2020).
[12] Y. Tsay, K. Ananthanarayanan, P. Gielisse, S. Mitra. J. Appl. Phys., **43** (9), 3677 (1972).
[13] P. Alekseev, B. Borodin, M. Dunaevskii, A. Smirnov, V.Y. Davydov, S. Lebedev, A. Lebedev. Techn. Phys. Lett., **44** (5), 381 (2018).
[14] M. Kratzer, O. Dimitriev, A. Fedoryak, N. Osipyonok, P. Balaz, M. Balaz, M. Tesinsky, C. Teichert. J. Appl. Phys., **125** (18), 185305 (2019).
[15] G. Shao. Energy Environ. Mater., **4** (3), 273 (2021).
[16] S. Ferrie, N. Darwish, J.J. Gooding, S. Ciampi. Nano Energy, **78**, 105210 (2020).
[17] W.N. Hansen, G.J. Hansen. Surf. Sci., **481** (1), 172 (2001).
[18] L. Diederich, O. Küttel, P. Aebi, L. Schlapbach. Surf. Sci., **418** (1), 219 (1998).
[19] P.A. Alekseev, V.A. Sharov, B.R. Borodin, M.S. Dunaevskiy, R.R. Reznik, G.E. Cirlin. Micromachines, **11** (6), 581 (2020).

Translated by Ego Translating